



## OPEN ACCESS

EDITED BY  
Jason Upton,  
Auburn University, United States

REVIEWED BY  
Karine Crozat,  
INSERM UMR1236 Microenvironnement,  
Différenciation cellulaire, Immunologie et  
Cancer, France  
Martin Messerle,  
Hannover Medical School, Germany

\*CORRESPONDENCE  
Sebastian Voigt  
✉ sebastian.voigt@uk-essen.de


†PRESENT ADDRESS  
Julia Cecilia Madela-Mönchinger,  
Miltenyi Biotec, Berlin, Germany

RECEIVED 22 March 2023  
ACCEPTED 27 October 2023  
PUBLISHED 23 November 2023

CITATION  
Madela-Mönchinger JC, Wolf SA, Wyler E,  
Bauer A, Mischke M, Möller L,  
Juranić Lisnić V, Landthaler M,  
Malyshkina A and Voigt S (2023) Rat  
cytomegalovirus efficiently replicates in  
dendritic cells and induces changes  
in their transcriptional profile.  
*Front. Immunol.* 14:1192057.  
doi: 10.3389/fimmu.2023.1192057

COPYRIGHT  
© 2023 Madela-Mönchinger, Wolf, Wyler,  
Bauer, Mischke, Möller, Juranić Lisnić,  
Landthaler, Malyshkina and Voigt. This is an  
open-access article distributed under the  
terms of the [Creative Commons Attribution  
License \(CC BY\)](https://creativecommons.org/licenses/by/4.0/). The use, distribution or  
reproduction in other forums is permitted,  
provided the original author(s) and the  
copyright owner(s) are credited and that  
the original publication in this journal is  
cited, in accordance with accepted  
academic practice. No use, distribution or  
reproduction is permitted which does not  
comply with these terms.

# Rat cytomegalovirus efficiently replicates in dendritic cells and induces changes in their transcriptional profile

Julia Cecilia Madela-Mönchinger<sup>1†</sup>, Silver Anthony Wolf<sup>2</sup>,  
Emanuel Wyler<sup>3</sup>, Agnieszka Bauer<sup>1</sup>, Marius Mischke<sup>4</sup>,  
Lars Möller<sup>5</sup>, Vanda Juranić Lisnić<sup>6</sup>, Markus Landthaler<sup>3</sup>,  
Anna Malyshkina<sup>4</sup> and Sebastian Voigt<sup>1\*</sup> 

<sup>1</sup>Department of Infectious Diseases, Robert Koch Institute, Berlin, Germany, <sup>2</sup>Genome Competence Center, Department of MFI, Robert Koch Institute, Berlin, Germany, <sup>3</sup>Laboratory for RNA Biology, Berlin Institute for Medical Systems Biology (BIMSB), Max Delbrück Center for Molecular Medicine in the Helmholtz Association (MDC), Berlin, Germany, <sup>4</sup>Institute for Virology, University Hospital Essen, University of Duisburg-Essen, Essen, Germany, <sup>5</sup>Advanced Light and Electron Microscopy, Robert Koch Institute, Berlin, Germany, <sup>6</sup>Center for Proteomics, University of Rijeka, Faculty of Medicine, Rijeka, Croatia

Dendritic cells (DC) play a crucial role in generating and maintaining antiviral immunity. While DC are implicated in the antiviral defense by inducing T cell responses, they can also become infected by Cytomegalovirus (CMV). CMV is not only highly species-specific but also specialized in evading immune protection, and this specialization is in part due to characteristic genes encoded by a given virus. Here, we investigated whether rat CMV can infect XCR1<sup>+</sup> DC and if infection of DC alters expression of cell surface markers and migration behavior. We demonstrate that wild-type RCMV and a mutant virus lacking the  $\gamma$ -chemokine ligand *xcl1* ( $\Delta vxcl1$  RCMV) infect splenic rat DC *ex vivo* and identify viral assembly compartments. Replication-competent RCMV reduced XCR1 and MHCII surface expression. Further, gene expression of infected DC was analyzed by bulk RNA-sequencing (RNA-Seq). RCMV infection reverted a state of DC activation that was induced by DC cultivation. On the functional level, we observed impaired chemotactic activity of infected XCR1<sup>+</sup> DC compared to mock-treated cells. We therefore speculate that as a result of RCMV infection, DC exhibit diminished XCR1 expression and are thereby blocked from the lymphocyte crosstalk.

## KEYWORDS

cytomegalovirus, dendritic cells, transcriptome, chemokines, XCL1, XCR1

**Abbreviations:** DC, dendritic cells; RCMV, Rat Cytomegalovirus; GPCR, G protein-coupled receptor.

## Introduction

During immunosuppression, opportunistic pathogens such as cytomegalovirus (CMV) contribute to increased morbidity and mortality. Due to its large genome bearing several immunomodulatory genes, CMV has the capacity to interfere with numerous immune cell types including dendritic cells (DC) (1–6).

As major antigen-presenting cells, DC link the innate and the adaptive immune response and play a central role in the activation of naïve T cells that are needed to neutralize invading pathogens (7). DC are crucial in the fight against viruses, and therefore, it is not surprising that they are targeted by different viral species. While conventional DC (cDC) can be infected with a multitude of viruses, plasmacytoid DC (pDC) resist most viral infections (8). Viruses targeting cDC include measles virus, influenza virus, HIV, hepatitis B and C viruses (9, 10), herpes simplex virus (11), CMV (12), and Varicella zoster virus (13), among others. Infection with measles virus abrogates the DC's ability to stimulate the proliferation of naïve allogeneic CD4<sup>+</sup> T cells (14). By contrast, influenza virus-infected DC were reported to induce a strong cytotoxic T cell response (15). Moreover, HIV exploits DC for dissemination to access other organs or cells (16, 17). Upon DC infection with murine CMV (MCMV), antigen uptake is impaired, DC phenotype is altered, and DC markers are downregulated (2). MCMV replicates productively in DC, recirculates with the help of M33, a virus-encoded chemokine receptor (18), and reaches the salivary gland via DC following intraperitoneal infection (19, 20). Hence, MCMV can remain in and modulate DC to escape an immune response.

While antigen presentation by MHC class I (MHCI) molecules to CD8<sup>+</sup> T cells reports intracellular events, presentation of antigen adopted from the extracellular milieu occurs by MHC class II (MHCI) to CD4<sup>+</sup> T cells. In addition, DC are able to present extracellularly acquired antigen by MHCI molecules to CD8<sup>+</sup> T cells, a process known as antigen cross-presentation (21). In mice, DC capable of cross-presenting antigen are characterized by the expression of XCR1, a G protein-coupled receptor, which represents a lineage marker for this specialized DC subset (22). XCR1 is predominantly co-expressed on CD8a<sup>+</sup> mouse cDC1 and CD141<sup>+</sup> human cDC1 (23, 24). In rats, splenic, thymic, and lymph node-derived DC have been characterized (25–27). In particular, splenic DC could be separated into CD4<sup>+</sup> and CD4<sup>-</sup> subsets, and unlike CD4<sup>-</sup> DC, CD4<sup>+</sup> DC expressed CD5, CD90, and SIRPα/CD172a (28, 29).

In previous work, we showed that CD4<sup>-</sup> XCR1<sup>+</sup> DC, but not CD4<sup>+</sup> XCR1<sup>-</sup> DC, are attracted by supernatants of rat embryo fibroblasts (REF) infected with wild-type but not *Δvxcl1* rat CMV (RCMV (30)). So far, the only known  $\gamma$ -chemokine analogue *vxcl1* is encoded by the English (RCMV-E) and Berlin (RCMV-B) isolates of RCMV (31). vXCL1 has a sequence similarity of 63.2% (RCMV-E) and 65.5% (RCMV-B) to the amino acid sequence of endogenous rat XCL1, suggesting that it likely originated from a co-evolutionary adaptation process between the virus and the host (31). Since vXCL1 is exclusively attracting XCR1<sup>+</sup> rat DC, we suggest that the virus manipulates this cell subset to evade the immune response.

Here, we extended previously reported rat DC analyses (27–29) to include XCR1 as an additional surface expression marker. By means of cross-presentation, XCR1<sup>+</sup> DC can directly prime CD8 T cells, and this represents a promising approach for vaccine strategies against tumors (32). To better understand how RCMV manipulates DC and if these strategies can be extended into the field of antiviral approaches, we investigated whether or not RCMV is able to infect and replicate in isolated splenic DC. Finally, we analyzed DC phenotypes and determined transcriptional profiles by bulk RNA-sequencing.

## Materials and methods

### Preparation of single cell suspensions and enrichment of rat DC from spleens

Sprague Dawley rats were bred at the animal facility of the Robert Koch Institute and sacrificed by an isoflurane overdose. To obtain single cell suspensions, spleens were homogenized using a gentleMACS dissociator (Miltenyi Biotec). To increase DC yields, homogenates were digested with 500  $\mu$ g/ml collagenase D, 20  $\mu$ g/ml DNase I and 2% (v/v) FCS in RPMI 1640 for 25 min in a 37°C water bath shaking at 200 rpm. Digestion was halted by the addition of 10 mM EDTA for 5 min under the same conditions. Cell suspensions were filtered through a 100  $\mu$ m nylon sieve (Becton Dickinson). After centrifugation at 380 x g for 8 min at 4°C, cells were applied to NycoPrep (PROGEN) or OptiPrep (PROGEN) density gradient centrifugation (density: 1.073 g/ml) at 1700 x g for 10 min at 4°C without applying de-acceleration. Lymphocytes were recovered from the NycoPrep/OptiPrep fractions and washed twice with MACS-PBS. To enrich OX-62-labeled cells, NycoPrep- or OptiPrep-enriched spleen cells were incubated with OX-62 microbeads (Miltenyi Biotec) according to the manufacturer's instructions. To prevent unspecific Fc receptor binding, cells were incubated with rat gamma globulin (final concentration 45.2  $\mu$ g/ml, Jackson ImmunoResearch) for 5 min on ice. Magnetically labeled cells were applied to a MS column (Miltenyi Biotec) for positive selection.

### Viruses and infections

Generation of the mutant *Δvxcl1* RCMV is described in (30). Likewise, a recombinant RCMV carrying *egfp* adjacent to *E32* was created by homologous recombination in eukaryotic cells. Both recombinant viral genomes were completely sequenced to rule out adventitious mutations that might have occurred during the recombination procedure, and none of such mutations were detected.

OX-62-enriched splenic DC were infected *ex vivo* with the respective viruses in chemotaxis medium (1x RPMI 1640, 1% [w/v] BSA [low-endotoxin; Gemini Bio-products], 100 U/ml Penicillin, 0.1 mg/ml Streptomycin, 50  $\mu$ M  $\beta$ -mercaptoethanol) at MOI 3. Virus was UV-inactivated at 1 J/cm<sup>2</sup> in 300  $\mu$ l on a 6-well plate.

Following OX-62 isolation, DC were either directly analyzed (input control) without cultivation or mock-infected and cultivated for 24 h before analysis.

## Antibodies and flow cytometry

Monoclonal antibodies (mAb) against RCMV-E immediate early 1 (IE1) protein were generated at the Center for Proteomics (University of Rijeka). Coupling of mAb to Alexa647 was conducted using a PD-10 desalting column (GE HealthCare). To characterize splenocytes, the following mAb were used: CD45RA (OX-33), CD54 (1A29), CD86 (24F), signal regulatory protein (SIRP) $\alpha$ /CD172a (OX-41), CD4 (W3/25), XCR1 (ZET), CD11b/c (OX-42), CD103 (OX-62; all from BioLegend); MHCII (OX-6) and CD103 (OX-62; both from BD Pharmingen); CD3 (REA227) and CD8a (REA437; both from Miltenyi Biotec). Titration of mAb was conducted for optimal signal-to-noise-ratio. Unspecific Fc receptor binding was inhibited by preincubation of cells with rat gamma globulin. Standard staining with mAb was performed in PBS containing 2% (v/v) FCS and 0.1% (w/v) NaN<sub>3</sub> for 20 min on ice. For intracellular IE1 staining, OX-62-enriched DC were stained with the LIVE/DEAD Fixable Orange Viability staining kit (Thermo Fisher Scientific) and fixed with 2% (w/v) PFA. Permeabilization was conducted with 0.5% saponin. Data were acquired on flow cytometers (Fortessa, Becton Dickinson and MACSQuant10, Miltenyi Biotec) and evaluated using FlowJo software v10.4.2 (Tree Star).

## Chemotaxis assays

Chemotaxis assays were conducted as described in (33). Briefly,  $2 \times 10^5$  DC were added to the upper chamber of a Transwell system. Each Transwell contained 100 ng/ml ( $1 \times 10^{-8}$  M) rXCL1 or no chemokine in the lower chamber. After 2.5 h of incubation, cells that had migrated to the lower chamber were analyzed by flow cytometry. CD3<sup>+</sup> and CD45RA<sup>+</sup> cells were excluded by gating and MHCII<sup>+</sup> CD103<sup>+</sup> CD4<sup>-</sup> XCR1<sup>+</sup> DC were examined for migration. Cells were counted over 5 min and the percentage of migrated cells was calculated by dividing the number of migrated cells by the number of input cells  $\times$  100.

## Transmission electron microscopy

RCMV-infected DC were fixed with 2.5% (w/v) glutaraldehyde in 50 mM HEPES, pH 7.2, harvested by scraping, pelleted at 2000  $\times$  g for 5 min at 4°C, and washed twice with HEPES. After washing, cells were block-embedded by mixing equal amounts of centrifuged cells and low-melting-agarose (3%). Agarose-embedded cells were cut into small pieces (<1 mm) and postfixated with osmium tetroxide (1% in double distilled H<sub>2</sub>O for 1 h), tannic acid (0.1% in 50 mM HEPES for 30 min) and uranyl acetate (2% in ddH<sub>2</sub>O for 2 h). Agarose-embedded cells were dehydrated in a gradient series of ethanol and propylene oxide and finally embedded in Epon resin.

Ultrathin sections (60 – 70 nm) were cut on a Leica-Ultracut ultramicrotome, mounted on naked 300 mesh copper grids, and counterstained with uranyl acetate (2% in ddH<sub>2</sub>O for 20 min), followed by lead citrate (Reynolds' solution for 3 min). Ultrathin sections were stabilized with a thin layer of carbon evaporation and examined using a JEM-2100 transmission electron microscope (JEOL) at 200 kV. Images were recorded using a Veleta CCD camera (EMSIS).

## Fluorescent microscopy

REF cells were infected with supernatants acquired from GFP-encoding RCMV-, GFP-encoding RCMV UV-, and mock-infected primary DC cultures and subjected to fluorescent microscopy five days later. Microscopic images were collected with a Leica Thunder Imager (Leica Microsystems UK Limited, Milton Keynes, UK).

## RNA isolation and sequencing

Cultured and infected (MOI 3, 24 hours post infection; hpi) DC were prepared in triplicates. RNA was extracted using Trizol (Thermo Fisher Scientific) and purified from the aqueous phase using the RNA Clean & Concentrator 25 kit (Zymo Research). For sequencing, poly(A) RNA was extracted from OX-62-enriched DC using the Dynabeads mRNA DIRECT Kit (Thermo Fisher Scientific). Sequencing libraries were prepared using the NEXTflex Directional RNA-Seq Kit dUTP-based (Bioo Scientific) and sequenced on an Illumina HiSeq 2000 device to generate single end reads of 50bp length. After initial quality control (QC), including trimming of the adapter sequence AGATCGGAAGAGCACACGT, approximately 25–30 million mappable reads were obtained per sample. Raw sequencing reads were aligned to version rn6 of the rat genome using hisat2 (34), and reads quantified against the version 93 Ensembl annotation using quasR (35). Differential expression analysis was then performed using edgeR (36).

## Quantitative RT-PCR

RNA was extracted from OX-62-enriched DC using innuPREP RNA Mini kit 2.0 and DNA removed by DNase I digestion. Of note, RNA amounts and integrity could not be assessed due to limited material, except for input samples. For those, around 20 ng RNA were isolated with a RIN >7. Subsequently, RNA was reverse transcribed using SuperScript III (ThermoFisher) with random hexamer priming according to the manufacturer's protocol. For detection, cDNA was amplified using the 2x SYBR green PCR master mix (ThermoFisher) with standard conditions. The following (in case of spliced genes, exon-spanning) forward and reverse primer were used: 5'-ACGTGACATGGACTCAGACT-3' and 5'-ACAAAACCAGGCTGTACCCA-3' (Rattus norvegicus Xcr1, Genbank acc. no. NM\_001106871.1); 5'-ACCTCAGCTACAGGACGGAC-3' and 5'-ATAGTCTCATTCCACCCAGTGC-3' (ifnb1, NM\_019127.2); 5'-TACCCTCTGTGGTTCCAGC-3'

and 5'-TCCTTTGGTTTCTTGACCACCT-3' (cd40; NM\_13436 0.1); 5'-GGGCTCCTCTGAATCGACTG-3' and 5'-GGCTACAC CCAAGAGCTTC-3' (cdc25a; D16236.1); 5'-TCCTATGCCTC ACAGATCCCA-3' and 5'-AGGGTGCTTATGCACGTCTG-3' (ccl6; NM\_001004202.3). The housekeeping gene peptidylprolyl isomerase A (Ppia; 5'-TCTGCACTGCCAAGACTGAG-3' and 5'-GTCCACAGTCGGAGATGGTG-3'; NM\_017101.1) was used to normalize the data using the  $\Delta\Delta$  Ct method (37).

## Results

### Two major DC populations in the spleen can be identified by CD103 and CD4 staining

In order to investigate the permissiveness of rat DC in RCMV infection, we initially defined a strategy to characterize DC subsets in spleens from Sprague Dawley rats. Splenocytes from ten-week-old rats were freshly isolated and enriched by OptiPrep density centrifugation and analyzed by flow cytometry. After isolating CD103<sup>+</sup> DC and gating on this population, we used MHCII expression levels to identify four DC subsets: CD4<sup>-</sup> MHCII<sup>+</sup>, CD4<sup>-</sup> MHCII<sup>++</sup>, CD4<sup>+</sup> MHCII<sup>+</sup>, and CD4<sup>+</sup> MHCII<sup>++</sup> DC. Based on CD4 expression, we further identified two major DC populations: MHCII<sup>+/++</sup> CD103<sup>+</sup> CD4<sup>-</sup> and MHCII<sup>+/++</sup> CD103<sup>+</sup> CD4<sup>+</sup> DC. These markers were then used to differentiate between two DC subpopulations: a) MHCII<sup>+</sup> CD103<sup>+</sup> CD11b/c<sup>+</sup> CD4<sup>+</sup> SIRP $\alpha$ /CD172a<sup>+</sup> XCR1<sup>-</sup>; and b) MHCII<sup>+</sup> CD103<sup>+</sup> CD11b/c<sup>+</sup> CD4<sup>-</sup> SIRP $\alpha$ /CD172a<sup>-</sup> XCR1<sup>+</sup> (Figure 1). CD11b/c, CD54 and, to a lesser extent, CD86 could be detected on both DC subsets, while SIRP $\alpha$ /CD172a was strongly expressed on the CD4<sup>+</sup> and dim on the CD4<sup>-</sup> subset. In contrast to mouse DC, CD8 expression remained undetected on rat spleen-derived DC. XCR1 was almost exclusively present on CD4<sup>-</sup> SIRP $\alpha$ /CD172a<sup>-</sup> DC. In all cell preparations, the purity of CD4<sup>-</sup> MHCII<sup>+</sup> cells used for viability or chemotaxis assays was above 85%.

### RCMV infects and replicates in splenic DC *ex vivo*

Since DC play a central role in the initiation and regulation of immune responses during CMV infection, we investigated the permissiveness and cellular response of DC to RCMV infection. After infection of freshly OX-62-isolated splenic DC from 10-week-old rats with wild-type and  $\Delta vxcl1$  RCMV, we could not observe a pronounced impact on cell viability, as assessed by LIVE/DEAD Fixable Orange Viability staining (Figure 2A). After 8, 16, and 24 hpi, the percentage of viable cells remained consistently higher in mock- than in RCMV-infected cells, albeit no drastic difference was observed. However, cultivation of DC was limited to 48 h because viability decreased to 40% (data not shown). To document viral infection, we measured expression of RCMV IE1 protein at 8, 16 and 24 hpi. Eight hpi, infection of CD103<sup>+</sup> DC was detected, and similar IE1 expression was seen after infection with both viruses 24 hpi (Figure 2B). As IE1 detection might not indicate replication-competent virus but merely an abortive infection, we assessed

productive viral infection of DC by electron microscopy 24 hpi. We identified cytoplasmic virus factories after nuclear egress (Figure 2C) as well as mature particles outside the cell (Figures 2D, E). These data were also confirmed by using a recombinant RCMV carrying an *egfp*-cassette adjacent to E32 and an UV-inactivated virus. As expected, infection with the *egfp*-containing virus resulted in a positive EGFP signal, while the UV-inactivated virus lacked GFP signal expression (Figure 2F). Moreover, wild-type RCMV-infected DC released infectious virus particles since supernatants collected from these DC infected REF cells (Figure 2G).

### RCMV infection affects DC phenotype and chemotactic activity

Having shown that RCMV can productively infect DC, we investigated the impact on phenotype and motility changes. Both wild-type and  $\Delta vxcl1$  mutant virus infection led to a strong reduction in XCR1 surface expression (Figure 3A). In contrast to mock infection, RCMV wild-type and  $\Delta vxcl1$  mutant virus-infected DC showed significantly decreased XCR1 expression at 8 and 24 hpi. Further, we observed reduced MHCII expression at 16 hpi and 24 hpi (Figure 3B). To examine whether RCMV infection impairs functional properties, we tested the chemotactic activity of DC 4 hpi in a transwell assay in the presence or absence of 100 ng/ml recombinant rXCL1. While mock-infected CD4<sup>-</sup> XCR1<sup>+</sup> DC migrated toward recombinant chemokine, both wild-type and  $\Delta vxcl1$  RCMV-infected DC failed to migrate. Likewise, cell movement did not occur in the absence of recombinant rXCL1 (Figure 3C). As a control, infection of CD4<sup>+</sup> DC did not exhibit chemotactic activity, irrespective of rXCL1 addition, as expected (Figure 3D).

### Cultivation and RCMV infection of DC induce changes in their transcriptional profile

As we could detect changes in the expression of selected DC surface molecules like XCR1 and MHCII by flow cytometry after RCMV infection, we extended our analyses to examining the whole transcriptome of RCMV-infected DC. As cultivation of isolated DC itself might induce transcriptomic changes, we initially compared the transcriptome profiles of freshly OX-62-isolated, uncultured, mock-infected CD4<sup>-</sup> CD172a<sup>-</sup> DC with mock-infected, 24 h cultured CD4<sup>-</sup> CD172a<sup>-</sup> DC.

Indeed, mere cultivation of rat splenic DC changed their transcriptomic profile, as compared with freshly isolated DC, suggesting that DC become activated during cultivation (Figure 4A, input vs. mock). Following cultivation, 2068 and 2505 genes out of about 11000 genes were significantly ( $p < 10^{-6}$ ) and at least 2-fold up- or downregulated, respectively (i.e., log(2) transformed fold change larger than one/less than minus one; Supplementary Table 1). Upregulated genes with higher expression following cultivation (i.e., higher in “mock” compared to “input” condition) included signaling proteins related to DC

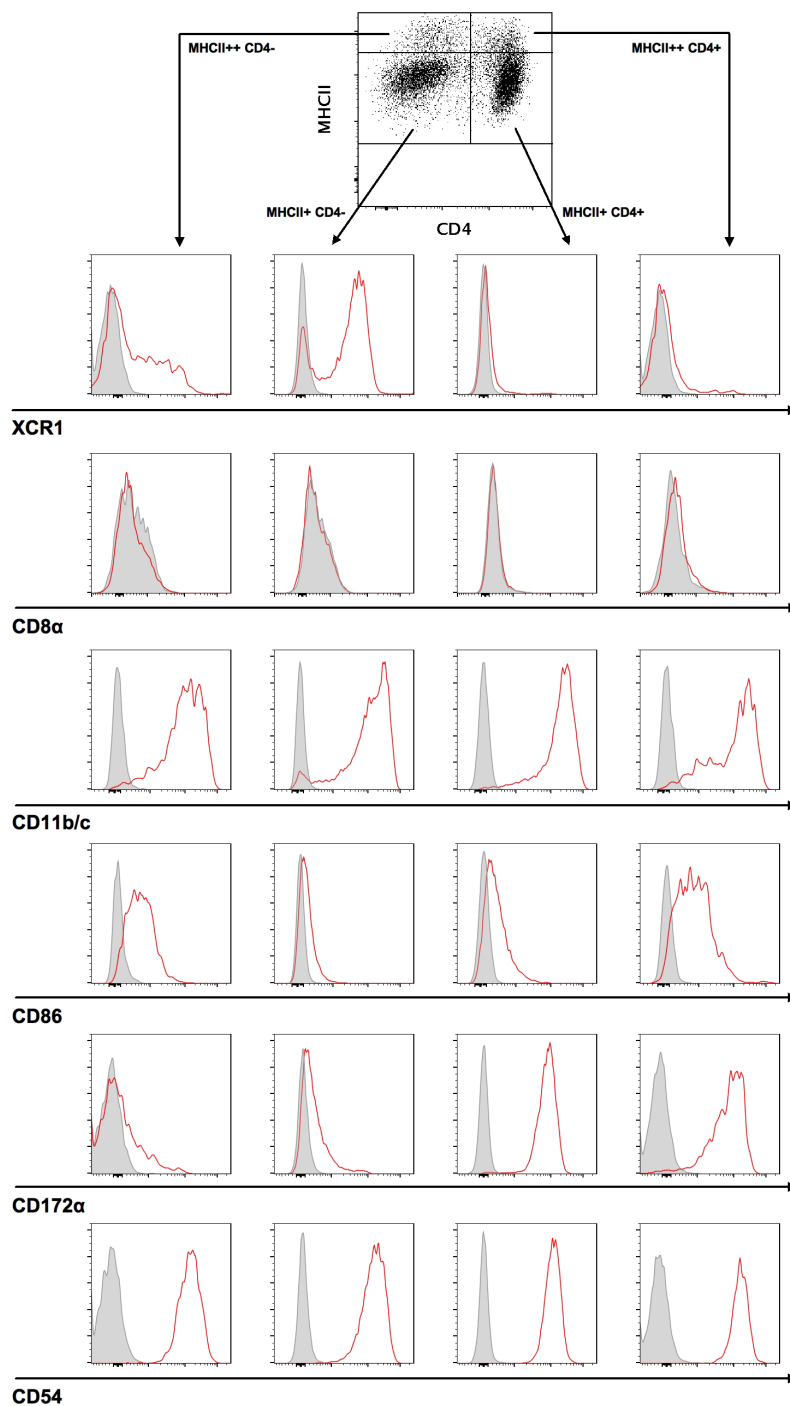


**FIGURE 1**  
 Two major DC subsets can be identified in splenocytes. For the characterization of DC subsets, splenocytes were stained with a target cell antibody panel and analyzed by flow cytometry. Cells were initially gated on singlets and live cells, followed by gating on CD3<sup>-</sup> CD45RA<sup>-</sup> CD103<sup>+</sup> DC. Next, CD103<sup>+</sup> DC were differentiated using MHCII and CD4 antibodies, divided into MHCII<sup>++</sup> or MHCII<sup>+</sup> and CD4<sup>+</sup> or CD4<sup>-</sup> DC, and subsequently characterized by antibody staining of XCR1, CD8α, CD11b/c, CD86, CD172α, and CD54. Representative histograms (red curve) for each analyzed surface marker are shown compared to a fluorescence minus one (FMO) control (grey curve).

migration such as *Pik3ca* and *Akt3* as well as maturation markers such as *Cd86*, *Cd80*, *Cd40*, and *Ccr7*. In contrast, XCR1 mRNA was barely detectable 24 h after incubation at 37°C in all sample groups (Figure 4A, Supplementary Table 1). This ligand-independent reduction of XCR1 mRNA confirmed the observed diminishment in surface expression, as shown above.

Next, we performed an unbiased gene set enrichment analysis with the genes that show differential expression between the different conditions (Figure 4B). Among the terms with the strongest signal were interferon response, complement, as well as two terms related to cell cycle (“E2F targets” and “G2-M checkpoint”). We then investigated five of these terms more closely. For each of them, we



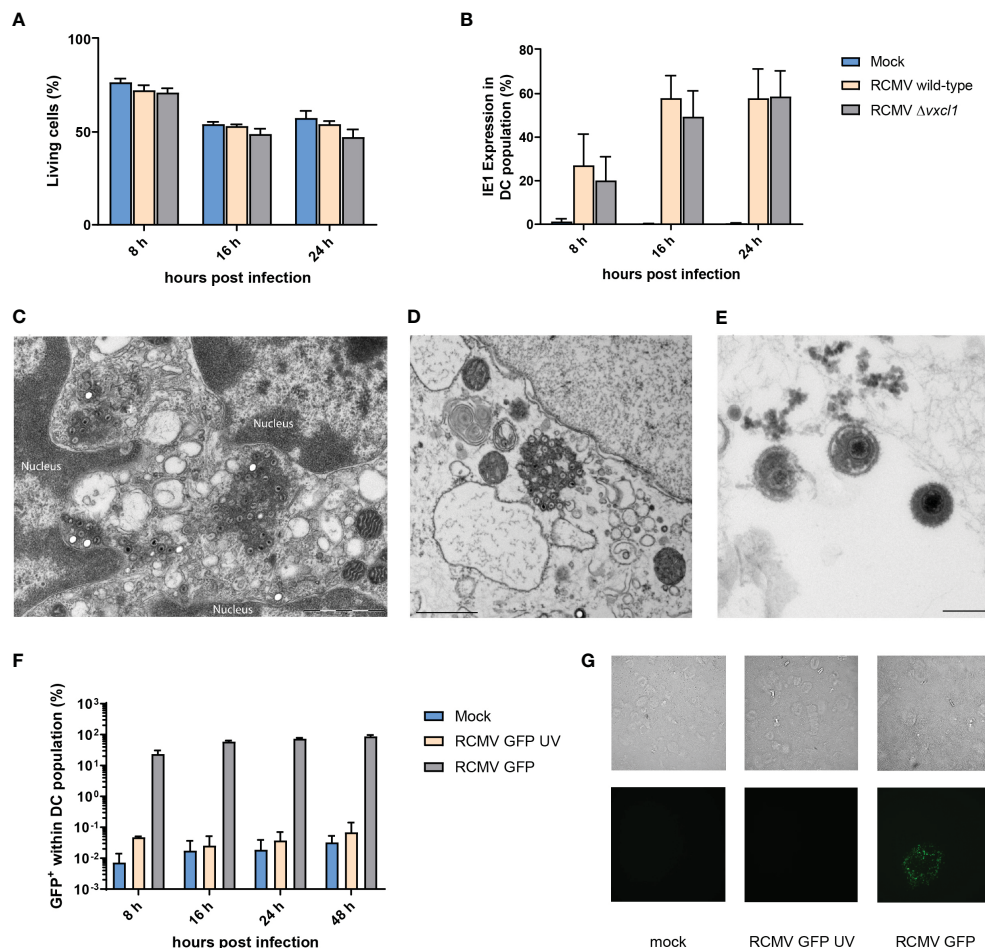


FIGURE 2

Viability of OX-62-enriched DC after infection with wild-type and  $\Delta xcl1$  RCMV and identification of replication compartments. DC were analyzed after 8, 16, and 24 hpi. (A) OX-62-enriched DC were infected with wild-type or  $\Delta xcl1$  RCMV. Mock-infected cells served as a negative control. (B) Expression of intracellular IE1 was analyzed by flow cytometry. Twenty-four hours post infection, ultrathin section transmission electron microscopy from OX-62-enriched DC revealed (C) viral capsids originating from cytoplasmic virus factories after nuclear egress and (D, E) mature viral particles outside the cell. (F) Recombinant GFP-encoding RCMV with or without UV inactivation. (G) Enriched DC were either mock-infected or infected with GFP-encoding RCMV with or without UV inactivation. Twenty-four hpi, supernatants were replaced with fresh culture medium. Forty-eight hours post initial infection, supernatants were collected and used to infect a REF monolayer at 75–80% confluency. Representative microscopic images of methylcellulose-overlaid REF cells are shown (bright-field upper row, GFP fluorescence lower row, 20x magnification).

selected the five genes with the strongest deregulation after analysis of all comparisons (e.g., mock vs. input, wild-type vs. mock etc; Figure 4C). First, we observed that genes that were upregulated in mock-infection vs. input were frequently downregulated in both wild-type and  $\Delta xcl1$  virus infections, such as cytokine-encoding *Cxcl11*, or *Fdft1* and *Fdps*, which are both coding for enzymes in the cholesterol synthesis pathway (Figure 4B). Vice versa, genes downregulated in comparing mock-infection vs. input, such as the MAP kinase target gene *Fosb*, were upregulated in infections compared vs. mock. For these genes, UV-inactivated virus-infected DC showed gene expression levels much closer to mock-infection. This “reversing pattern”, i.e., that changes in gene expression induced by the cultivation of DC were reverted by RCMV infection, was also observed for cell cycles genes (Figure 4C, top panel). In addition, we found that genes upregulated in mitosis such as *Top2a*, *Cenpe* or *Ube2c* exhibited stronger expression in infected

DC, indicating that these genes contribute to cell division (Supplementary Figure 1A). Second, differences between mock- and UV-inactivated virus-infected DC were considerably smaller than those between non-inactivated virus and mock-infections. UV-inactivated virus is unable to replicate and cannot initiate large parts of its gene expression program. Accordingly, we detected substantial differences between wild-type and UV-irradiated RCMV infection (Figure 5). Differences in DC gene expression after wild-type and  $\Delta xcl1$  RCMV infection were comparatively small, with only about 50 genes showing significant differences and reproducible expression patterns (Supplementary Figure 1B).

To validate our RNA-Seq results, we newly isolated DC from two rats and performed quantitative RT-PCR based on a set of genes that cover different terms including cell cycle and innate immunity pathways. Messenger RNA was extracted from OX-62-sorted DC that were either mock-infected, UV-infected, infected

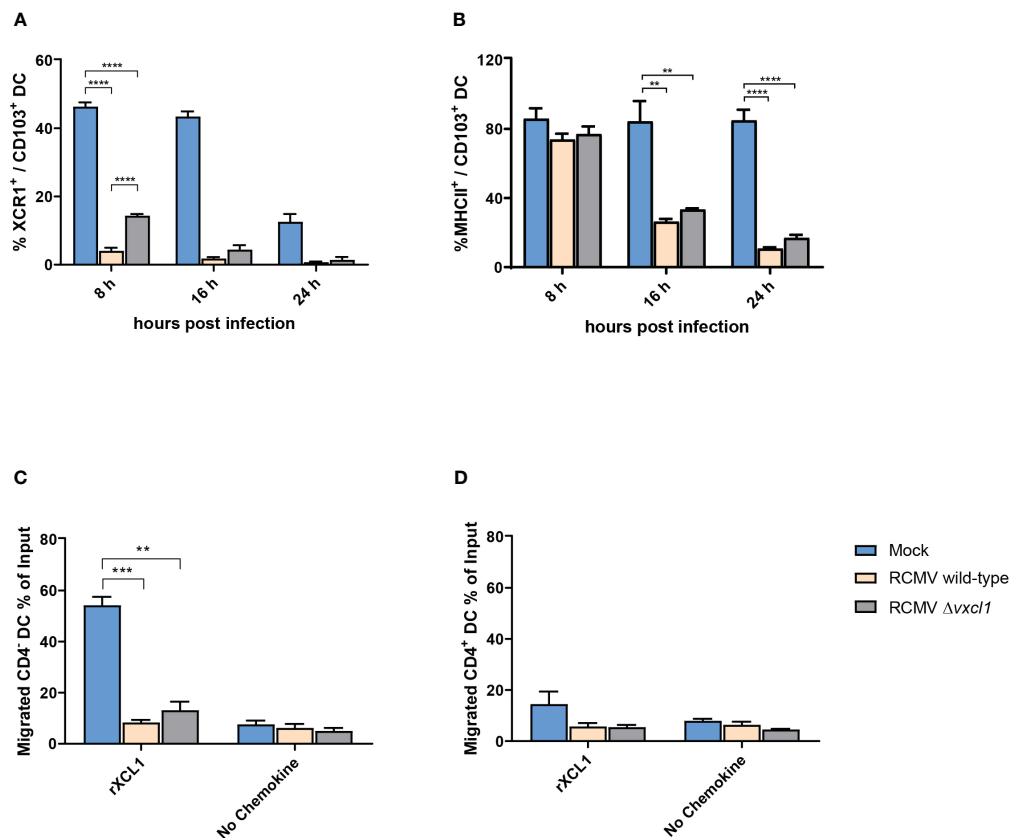


FIGURE 3

Analysis of DC surface markers and migration of CD4 DC after infection with RCMV. DC were analyzed after 8, 16, and 24 hpi. OX-62-enriched DC were infected with wild-type or  $\Delta vxcl1$  RCMV. Mock-infected cells served as a negative control. XCR1 (A) and MHCII (B) were stained. Migration of CD4<sup>+</sup> (C) and CD4<sup>+</sup> (D) DC were analyzed in the presence or absence of recombinant rat XCL1 (rXCL1). Error bars represent mean  $\pm$  SD, n=3 independent experiments. \*\* p<0.001; \*\*\* p<0.0001; \*\*\*\* p<0.00001; (one-way ANOVA and Dunnett's multiple comparison test).

with wild-type, or  $\Delta vxcl1$  RCMV *in vitro*. Xcr1, Ifnb1, Cd40; Cdc25a, and Ccl6 mRNA were quantified and compared to input DC mRNA as a reference. The housekeeping gene peptidylprolyl isomerase A (Ppia) was used as a reference gene for normalization of quantitative RT-PCR data. The RT-PCR results could mostly recapitulate the data obtained with the RNA-Seq approach, although input values were generally higher in RT-PCR analyses (Figure 5, Supplementary Figure 2).

## Discussion

Initially, we performed a phenotypic characterization of rat DC and identified two main DC subsets in the spleen: MHCII<sup>+</sup> CD103<sup>+</sup> CD11b/c<sup>+</sup> CD4<sup>+</sup> SIRP $\alpha$ /CD172a<sup>+</sup> XCR1<sup>-</sup> DC on the one hand and MHCII<sup>+</sup> CD103<sup>+</sup> CD11b/c<sup>+</sup> CD4<sup>-</sup> SIRP $\alpha$ /CD172a<sup>-</sup> XCR1<sup>+</sup> DC on the other. Thus, our data confirm previous results from rat DC studies (25–29), including the observation that, in contrast to murine DC, splenic rat DC lack CD8a expression (38). We added the GPCR XCR1, the  $\gamma$ -chemokine receptor, to include a marker that defines cross-presenting DC in mice and humans (39, 40). In rats, cross-presentation data of XCR1<sup>+</sup> DC are unpublished;

phenotypically, XCR1 appears to be almost exclusively expressed on CD4<sup>+</sup> rat DC.

Next, we analyzed DC viability under different conditions. Overall, freshly isolated DC (input), compared with wild-type and  $\Delta vxcl1$  RCMV-infected DC, did not exhibit major differences in viability at a given time point, but overall viability declined. Following MCMV infection, DC viability was also robust, however, a growth factor-dependent immature mouse DC line was used in that study (2, 41). Infection of DC with wild-type or  $\Delta vxcl1$  RCMV resulted in IE1 expression and in GFP expression after infection with a GFP-expressing recombinant virus. Here, we define DC infection not merely as the detection of viral IE1 or GFP expression as these could document successful entry but also an abortive infection; furthermore, infection should include the visualization of viral progeny. Successful viral replication could be confirmed by electron microscopy detection of capsids after nuclear egress and the identification of cytoplasmic virus factories. Moreover, primary DC cultures were productively infected since culture supernatants were infectious for REF.

RCMV is the only known virus to have evolved a  $\gamma$ -chemokine analogue, vXCL1, that engages its cognate receptor XCR1 and thereby attracts XCR1<sup>+</sup> DC (30, 31, 33). Like other CMV, RCMV

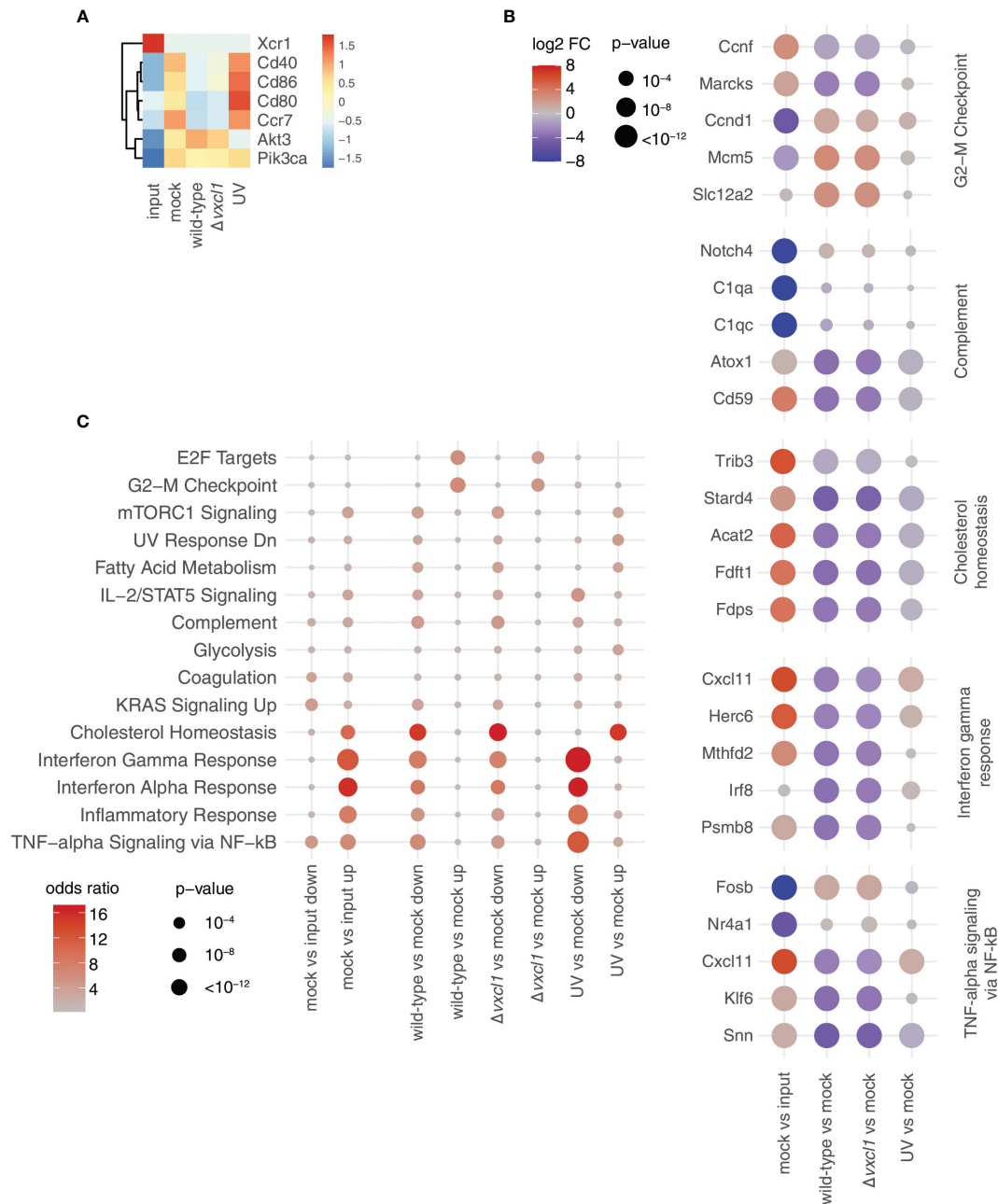


**FIGURE 4**  
 Transcriptomic changes upon DC cultivation and RCMV infection. **(A)** Expression values of the indicated DC markers for the five conditions analyzed are depicted as z-scores of normalized expression values (transcripts per million, tpm) averaged over three replicates from the RNA-seq data. **(B)** For the indicated comparisons, the top 500 up/downregulated genes, respectively, were used for gene set enrichment analysis using enrichR. For every gene set, the terms shown are the union of the five terms with the smallest adjusted p-values. Data are shown as dot plots with  $-\log_{10}$  transformed adjusted p-value as the size, and the  $\log_2$  transformed odds ratio (i.e., how many more genes are assigned to a term in the indicated gene set than expected) represented by the color. Rows are ordered according to an unsupervised clustering. For calculation of adjusted p-values, enrichR uses a hypergeometric test with FDR correction. **(C)** For selected terms, the five genes with the smallest p-values as calculated by the edgeR package used for differential expression analysis across all comparisons are indicated at the bottom. Values are shown as dotplots, with the size of the dot proportional to the  $-\log_{10}$  transformed p-values, and the color indicative of the  $\log_2$  transformed fold change. Within each term, genes are ordered according to an unsupervised clustering. For calculation of p-values, edgeR uses an exact two-sided binomial test.

encodes a number of immune evasion genes that might have prompted the host to employ cross-presentation, and RCMV might use vXCL1 to circumvent this strategy of the immune system. After CMV infection of cells that have become apoptotic, DC cross-present ingested viral antigens to CD8<sup>+</sup> T cells (42). This

feature might be impaired upon direct infection of DC, however, the permissiveness of cross-presenting DC might serve as an antiviral strategy to prime CD8<sup>+</sup> T cells (43). In addition to RCMV infection, DC function might be dampened by infected cells secreting vXCL1 that bind XCR1 and result in XCR1 downmodulation, thereby



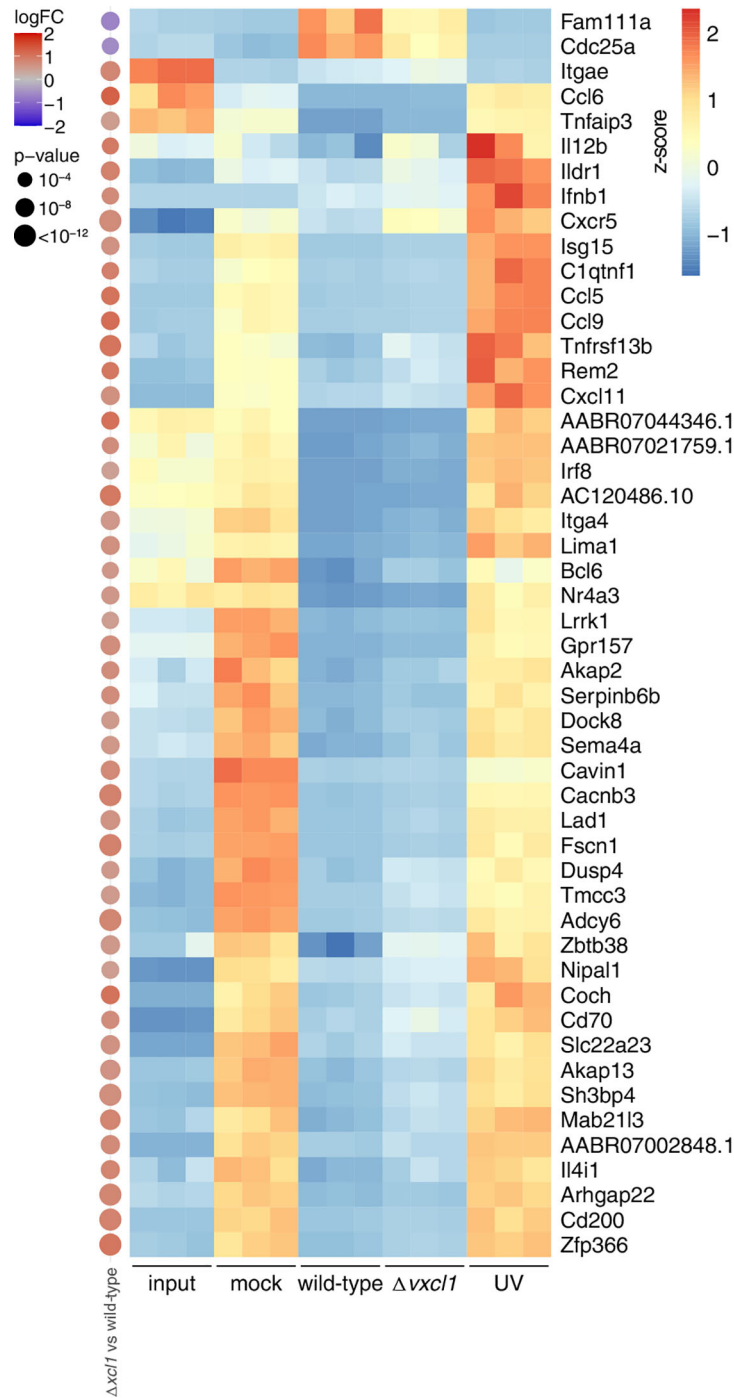


FIGURE 5

Transcriptomic changes upon infection with wild-type,  $\Delta vxcl1$ , and UV-inactivated RCMV. Expression values of the indicated differentially expressed genes (top 50 differentially expressed of  $\Delta vxcl1$  RCMV compared to wild-type RCMV infection) are depicted as z-scores of normalized expression values (tpm) of the individual samples (replicates 1-3) in the RNA-Seq data. On the left, differential expression values as calculated by edgeR for  $\Delta vxcl1$  RCMV vs. wild-type RCMV are shown, with the size of the dot proportional to the  $-\log_{10}$  transformed p-values, and the color indicative of the  $\log_2$  transformed fold change. For calculation of p-values, edgeR uses an exact two-sided binomial test.

rendering this DC subset unresponsive. Also, vXCL1 might attract uninfected DC to facilitate viral dissemination, suggesting that vXCL1 (as XCL1) acts rather locally than over large distances.

Following infection with MCMV and the Maastricht isolate of RCMV, DC phenotypic changes including diminished MHCII expression have been reported (2, 44). Infection with RCMV-E

induced a similar reduction in MHCII expression that became profound 16 hours and 24 hpi. Likewise, we detected reduced XCR1 surface expression after RCMV infection that was visible already at 8 hpi. At this time point, XCR1 expression was less pronounced after infection with wild-type RCMV which might indicate that  $\Delta vxcl1$  RCMV could be less successful in attracting and

subsequently infecting DC. On the mRNA level, XCR1 was barely detectable after 24 h in all sample groups (data not shown), confirming our previous published results concerning the ligand-independent reduction of XCR1 expression (33). Both wild-type and  $\Delta vxcl1$  RCMV infection impeded migration of CD4<sup>+</sup> DC toward endogenous XCL1, thereby possibly interfering with DC recruitment by NK cells and CD8<sup>+</sup> T cells, as they constitute the main XCL1 source.

By comparing the transcriptomic profiles of uncultured DC with 24 h cultured DC, we sought to determine whether cultivation of isolated DC itself induced different patterns of gene expression. In our RNA-Seq analysis, we revealed major changes between DC that were either uncultured (“Input”) or mock-infected and cultured (“Mock”). Rat splenic DC became activated during cultivation, and maybe even during the isolation procedure including digestion, gradient centrifugation and microbead labeling, a phenomenon that has also been described for murine DC (2, 28, 45). Similarly, we observed decreased transcription of the maturation markers *Cd86*, *Cd80*, *Cd40*, and *Ccr7*, as after MCMV infection (2), suggesting that RCMV hampers DC maturation. *In vivo*, DC maturation is essential for the migration and initiation of T cell-derived immune responses. The inhibition of maturation might result in a paralyzed state and DC dysfunctionality, resulting in downstream T cell impairment, as has been described for herpes simplex virus, vaccinia virus and human CMV (46–48). In contrast, *Xcr1* was highly transcribed in uncultured cells. This transcriptional state flipped after 24 h of cultivation when *Xcr1* transcription became hardly detectable. Also, RCMV infection led to a rapid reduction of *Xcr1* transcription which is likely not only due to the infection process but also to XCR1 recycling (33).

After RCMV infection of cultured DC, 2001 and 1954 genes were significantly up- or downregulated, respectively, compared to mock-infection. We detected a substantial upregulation of genes involved in cell cycle and mitosis. However, upon DC cultivation, these genes were less abundantly expressed, which might suggest a G1 arrest in this condition that is reverted in infected cells. By contrast, several cytokines showed enhanced transcription only after mock-infection or infection with irradiated virus, possibly indicating the suppression of these genes upon viral encounter. In a published dataset, 130 murine and human DC genes were regulated upon maturation that contained putative transcription factor binding sites for IRF and NF- $\kappa$ B and therefore, maturation seems to be driven by genes controlled by IFN and NF- $\kappa$ B (49). In another study, transcriptomic changes were investigated in human myeloid DC after human CMV infection. Almost 200 genes were upregulated 6 hpi, and approximately 600 genes were upregulated and approximately 300 downregulated at 16 hpi (50).

To observe for changes in the DC transcriptomic profile, we compared wild-type virus to  $\Delta vxcl1$  RCMV infection. Overall, expression of DC genes after infection with wild-type and  $\Delta vxcl1$  RCMV were quite similar, yet there were about 50 genes that exhibited expression of significant difference. Among these were *Cxcr5*, *Il12b*, and *Cd200* that all play a role in antiviral immunity. As with rat DC, *Cd200* was also found to be upregulated in murine DC upon maturation (49). While both wild-type as well as  $\Delta vxcl1$

RCMV infection decrease *Cd200* transcription, lack of vXCL1 seems to allow for higher *Cd200* gene expression. Decreased CD200 expression on the DC surface might lead to DC tolerization and influence (v)XCL1 binding to XCR1, thereby impairing cross-presentation and subsequent T cell activation. Therefore, it can be speculated that RCMV employs vXCL1 to reduce CD200 abundance on DC.

Our RNA-seq data show that cultivation as well as RCMV infection of DC led to changes on the transcriptional level. We could detect similar changes in mRNA expression by quantitative RT-PCR for *Xcr1*, *Cdc25a*, and *Ccl6* and mainly for *Ifnb1* and *Cd40*. For *Ifnb1*, UV-treated RCMV showed highest expression as with RNA-seq, however, expression was detected in the mock-infected sample. For *Cd40*, mRNA expression was seen in the mock-infected but less in the UV-treated RCMV-infected sample. Generally, we detected high expression of input mRNA with RT-PCR that was not seen with RNA-seq. This might be due to the higher amount of mRNA detectable in the input sample as well as the difference of the two methods. While the results of the different infection conditions are comparable between the methods, this does not account for the input condition.

In summary, we show that maturation marker genes and genes regulating the cell cycle are affected by RCMV infection and identified different transcription profiles that depend on *vxcl1* transcription. Therefore, the analysis of the interaction between RCMV and XCR1<sup>+</sup> DC should shed further light on CMV-induced immunosuppression and might be useful to improve antiviral or antitumor therapies by targeting cross-presenting DC.

## Data availability statement

The data presented in the study are deposited in the NCBI GEO repository, accession number GSE232184.

## Author contributions

JCM-M, SW, LM, AB, MM, AM, and EW performed experiments. VJ and ML provided reagents. JCM-M, SW, EW, and AM analyzed the data. JCM-M, EW, and SV wrote the manuscript. SV supervised the project. All authors contributed to the article and approved the submitted version.

## Funding

This work was supported by the Deutsche Forschungsgemeinschaft (VO 774/7-2 to SV).

## Conflict of interest

The authors declare that the research was conducted in the absence of any commercial or financial relationships that could be construed as a potential conflict of interest.

## Publisher's note

All claims expressed in this article are solely those of the authors and do not necessarily represent those of their affiliated organizations, or those of the publisher, the editors and the reviewers. Any product that may be evaluated in this article, or claim that may be made by its manufacturer, is not guaranteed or endorsed by the publisher.

## Supplementary material

The Supplementary Material for this article can be found online at: <https://www.frontiersin.org/articles/10.3389/fimmu.2023.1192057/full#supplementary-material>

### SUPPLEMENTARY FIGURE 1

(A) Expression values of the indicated mitosis markers in the five conditions are depicted as z-scores of normalized expression values (tpm) averaged over

## References

- Alcami A, Koszinowski UH. Viral mechanisms of immune evasion. *Trends Microbiol* (2000) 8(9):410–8. doi: 10.1016/s0966-842x(00)01830-8
- Andrews DM, Andoniou CE, Granucci F, Ricciardi-Castagnoli P, Degli-Esposti MA. Infection of dendritic cells by murine cytomegalovirus induces functional paralysis. *Nat Immunol* (2001) 2(11):1077–84. doi: 10.1038/ni724
- Reeves MB, MacAry PA, Lehner PJ, Sissons JG, Sinclair JH. Latency, chromatin remodeling, and reactivation of human cytomegalovirus in the dendritic cells of healthy carriers. *Proc Natl Acad Sci U.S.A.* (2005) 102(11):4140–5. doi: 10.1073/pnas.0408994102
- Riegler S, Hebart H, Einsele H, Brossart P, Jahn G, Sinzger C. Monocyte-derived dendritic cells are permissive to the complete replicative cycle of human cytomegalovirus. *J Gen Virol* (2000) 81(Pt 2):393–9. doi: 10.1099/0022-1317-81-2-393
- Hertel L, Lacaille VG, Strobl H, Mellins ED, Mocarski ES. Susceptibility of immature and mature langerhans cell-type dendritic cells to infection and immunomodulation by human cytomegalovirus. *J Virol* (2003) 77(13):7563–74. doi: 10.1128/jvi.77.13.7563-7574.2003
- Miller-Kittrell M, Sparer TE. Feeling manipulated: cytomegalovirus immune manipulation. *Viol J* (2009) 6(1):4. doi: 10.1186/1743-422X-6-4
- Vyas JM, van der Veen AG, Ploegh HL. The known unknowns of antigen processing and presentation. *Nat Rev Immunol* (2008) 8(8):607–18. doi: 10.1038/nri2368
- Yun TJ, Igarashi S, Zhao H, Perez OA, Pereira MR, Zorn E, et al. Human plasmacytoid dendritic cells mount a distinct antiviral response to virus-infected cells. *Sci Immunol* (2021) 6(58):eabc7302. doi: 10.1126/sciimmunol.abc7302
- Arima S, Akbar SM, Michitaka K, Horiike N, Nuriya H, Kohara M, et al. Impaired function of antigen-presenting dendritic cells in patients with chronic hepatitis B: localization of HBV DNA and HBV RNA in blood DC by in situ hybridization. *Int J Mol Med* (2003) 11(2):169–74. doi: 10.3892/ijmm.11.2.169
- Navas MC, Fuchs A, Schvoerer E, Bohbot A, Aubertin AM, Stoll-Keller F. Dendritic cell susceptibility to hepatitis C virus genotype 1 infection. *J Med Virol* (2002) 67(2):152–61. doi: 10.1002/jmv.2204
- Kruse M, Rosorius O, Kratzer F, Stelz G, Kuhnt C, Schuler G, et al. Mature dendritic cells infected with herpes simplex virus type 1 exhibit inhibited T-cell stimulatory capacity. *J Virol* (2000) 74(15):7127–36. doi: 10.1128/jvi.74.15.7127-7136.2000
- Hahn G, Jores R, Mocarski ES. Cytomegalovirus remains latent in a common precursor of dendritic and myeloid cells. *Proc Natl Acad Sci U.S.A.* (1998) 95(7):3937–42. doi: 10.1073/pnas.95.7.3937
- Abendroth A, Morrow G, Cunningham AL, Slobedman B. Varicella-zoster virus infection of human dendritic cells and transmission to T cells: implications for virus dissemination in the host. *J Virol* (2001) 75(13):6183–92. doi: 10.1128/JVI.75.13.6183-6192.2001
- Grosjean I, Caux C, Bella C, Berger I, Wild F, Banchereau J, et al. Measles virus infects human dendritic cells and blocks their allostimulatory properties for CD4+ T cells. *J Exp Med* (1997) 186(6):801–12. doi: 10.1084/jem.186.6.801
- Bhardwaj N, Bender A, Gonzalez N, Bui LK, Garrett MC, Steinman RM. Influenza virus-infected dendritic cells stimulate strong proliferative and cytolytic responses from human CD8+ T cells. *J Clin Invest* (1994) 94(2):797–807. doi: 10.1172/JCI117399
- Wu L, KewalRamani VN. Dendritic-cell interactions with HIV: infection and viral dissemination. *Nat Rev Immunol* (2006) 6(11):859–68. doi: 10.1038/nri1960
- Langhoff E, Terwilliger EF, Bos HJ, Kalland KH, Poznansky MC, Bacon OM, et al. Replication of human immunodeficiency virus type 1 in primary dendritic cell cultures. *Proc Natl Acad Sci U.S.A.* (1991) 88(18):7998–8002. doi: 10.1073/pnas.88.18.7998
- Farrell HE, Bruce K, Lawler C, Oliveira M, Cardin R, Davis-Poynter N, et al. Murine cytomegalovirus spreads by dendritic cell recirculation. *mBio* (2017) 8(5):e01264–17. doi: 10.1128/mBio.01264-17
- Farrell HE, Bruce K, Lawler C, Stevenson PG. Murine cytomegalovirus spread depends on the infected myeloid cell type. *J Virol* (2019) 93(15):e00540–19. doi: 10.1128/JVI.00540-19
- Farrell HE, Bruce K, Redwood AJ, Stevenson PG. Murine cytomegalovirus disseminates independently of CX3CR1, CCL2 or its M131/M129 chemokine homologue. *J Gen Virol* (2019) 100(12):1695–700. doi: 10.1099/jgv.0.001333
- Sigal LJ, Crotty S, Andino R, Rock KL. Cytotoxic T-cell immunity to virus-infected non-haematopoietic cells requires presentation of exogenous antigen. *Nature* (1999) 398(6722):77–80. doi: 10.1038/18038
- Bachem A, Hartung E, Guttler S, Mora A, Zhou X, Hegemann A, et al. Expression of XCR1 characterizes the Batf3-dependent lineage of dendritic cells capable of antigen cross-presentation. *Front Immunol* (2012) 3:214. doi: 10.3389/fimmu.2012.00214
- Gurka S, Hartung E, Becker M, Kroczeck RA. Mouse Conventional Dendritic Cells Can be Universally Classified Based on the Mutually Exclusive Expression of XCR1 and SIRPα. *Front Immunol* (2015) 6:35. doi: 10.3389/fimmu.2015.00035
- Bachem A, Guttler S, Hartung E, Ebstein F, Schaefer M, Tannert A, et al. Superior antigen cross-presentation and XCR1 expression define human CD11c+CD141+ cells as homologues of mouse CD8+ dendritic cells. *J Exp Med* (2010) 207(6):1273–81. doi: 10.1084/jem.20100348
- Hubert FX, Voisine C, Louvet C, Heslan JM, Ouabed A, Heslan M, et al. Differential pattern recognition receptor expression but stereotyped responsiveness in rat spleen dendritic cell subsets. *J Immunol* (2006) 177(2):1007–16. doi: 10.4049/jimmunol.177.2.1007
- Hubert FX, Voisine C, Louvet C, Heslan M, Josien R. Rat plasmacytoid dendritic cells are an abundant subset of MHC class II+ CD4+CD11b-OX62- and type I IFN-producing cells that exhibit selective expression of Toll-like receptors 7 and 9 and strong responsiveness to CpG. *J Immunol* (2004) 172(12):7485–94. doi: 10.4049/jimmunol.172.12.7485
- Trinite B, Chauvin C, Peche H, Voisine C, Heslan M, Josien R. Immature CD4-CD103+ Rat dendritic cells induce rapid caspase-independent apoptosis-like cell death in various tumor and nontumor cells and phagocytose their victims. *J Immunol* (2005) 175(4):2408–17. doi: 10.4049/jimmunol.175.4.2408
- Voisine C, Hubert F-X, Trinite B, Heslan M, Josien R. Two phenotypically distinct subsets of spleen dendritic cells in rats exhibit different cytokine production and T cell stimulatory activity. *J Immunol* (2002) 169(5):2284–91. doi: 10.4049/jimmunol.169.5.2284
- Trinite B, Voisine C, Yagita H, Josien R. A subset of cytolytic dendritic cells in rat. *J Immunol* (2000) 165(8):4202–8. doi: 10.4049/jimmunol.165.8.4202

### SUPPLEMENTARY FIGURE 2

Quantitative RT-PCR of mRNA extracted from OX-62-enriched DC from a total of two rats. After isolation and enrichment, DC were mock- or UV-infected or infected with wild-type or  $\Delta vxc1I$  RCMV (see colored bars). RT-PCR was carried out to quantitate Ccl6, Cd40, Cdc25a, Irfb1, and Xcr1 mRNA. Relative mRNA expression is shown on the ordinate. The housekeeping gene Ppia was used to normalize the data using the  $\Delta\Delta$  Ct method and input mRNA (red) was used as a reference to calculate  $\Delta\Delta$  Ct values. Averages and individual measurements of two rats each are shown. Error bars denote standard deviation.

### SUPPLEMENTARY TABLE 1

Differential expression values of mock-infected compared to input cells.

30. Geyer H, Hartung E, Mages HW, Weise C, Beluzic R, Vugrek O, et al. Cytomegalovirus expresses the chemokine homologue vxcl1 capable of attracting XCR1+ CD4- dendritic cells. *J Virol* (2014) 88(1):292–302. doi: 10.1128/JVI.02330-13
31. Geyer H, Ettinger J, Moller L, Schmolz E, Nitsche A, Brune W, et al. Rat cytomegalovirus (RCMV) English isolate and a newly identified Berlin isolate share similarities with but are separate as an anciently diverged clade from Mouse CMV and the Maastricht isolate of RCMV. *J Gen Virol* (2015) 96(Pt 7):1873–0. doi: 10.1099/vir.0.000109
32. Kroczek AL, Hartung E, Gurka S, Becker M, Reeg N, Mages HW, et al. Structure-Function Relationship of XCL1 Used for in vivo Targeting of Antigen Into XCR1+ Dendritic Cells. *Front Immunol* (2018) 9:2806. doi: 10.3389/fimmu.2018.02806
33. Bauer A, Madela J, Berg C, Daugvilaite V, Gurka S, Mages HW, et al. Rat cytomegalovirus-encoded gamma-chemokine vxcl1 is a highly adapted, species-specific agonist for rat XCR1-positive dendritic cells. *J Cell Sci* (2019) 133(5):jcs236190. doi: 10.1242/jcs.236190
34. Kim D, Paggi JM, Park C, Bennett C, Salzberg SL. Graph-based genome alignment and genotyping with HISAT2 and HISAT-genotype. *Nat Biotechnol* (2019) 37(8):907–15. doi: 10.1038/s41587-019-0201-4
35. Gaidatzis D, Lerch A, Hahne F, Stadler MB. QuasR: quantification and annotation of short reads in R. *Bioinformatics* (2015) 31(7):1130–2. doi: 10.1093/bioinformatics/btu781
36. McCarthy DJ, Chen Y, Smyth GK. Differential expression analysis of multifactor RNA-Seq experiments with respect to biological variation. *Nucleic Acids Res* (2012) 40(10):4288–97. doi: 10.1093/nar/gks042
37. Livak KJ, Schmittgen TD. Analysis of relative gene expression data using real-time quantitative PCR and the 2<sup>-</sup>( $\Delta\Delta C_T$ ) method. *Methods* (2001) 25(4):402–8. doi: 10.1006/meth.2001.1262
38. Yrlid U, Macpherson G. Phenotype and function of rat dendritic cell subsets. *APMIS* (2003) 111(7-8):756–65. doi: 10.1034/j.1600-0463.2003.11107807.x
39. Dorner BG, Dorner MB, Zhou X, Opitz C, Mora A, Güttler S, et al. Selective expression of the chemokine receptor XCR1 on cross-presenting dendritic cells determines cooperation with CD8+ T cells. *Immunity* (2009) 31(5):823–33. doi: 10.1016/j.immuni.2009.08.027
40. Crozat K, Guiton R, Contreras V, Feuillet V, Dutertre CA, Ventre E, et al. The XC chemokine receptor 1 is a conserved selective marker of mammalian cells homologous to mouse CD8alpha+ dendritic cells. *J Exp Med* (2010) 207(6):1283–92. doi: 10.1084/jem.20100223
41. Winzler C, Rovere P, Rescigno M, Granucci F, Penna G, Adorini L, et al. Maturation stages of mouse dendritic cells in growth factor-dependent long-term cultures. *J Exp Med* (1997) 185(2):317–28. doi: 10.1084/jem.185.2.317
42. Arrode G, Boccaccio C, Lule J, Allart S, Moinard N, Abastado JP, et al. Incoming human cytomegalovirus pp65 (UL83) contained in apoptotic infected fibroblasts is cross-presented to CD8+ T cells by dendritic cells. *J Virol* (2000) 74(21):10018–24. doi: 10.1128/jvi.74.21.10018-10024.2000
43. Freigang S, Probst HC, van den Broek M. Dc infection promotes antiviral CTL priming: the ‘Winkelried’ strategy. *Trends Immunol* (2005) 26(1):13–8. doi: 10.1016/j.it.2004.11.013
44. Baca Jones CC, Kreklywich CN, Messaoudi I, Vomaska J, McCartney E, Orloff SL, et al. Rat cytomegalovirus infection depletes MHC II in bone marrow derived dendritic cells. *Virology* (2009) 388(1):78–90. doi: 10.1016/j.virol.2009.02.050
45. Vremec D, Pooley J, Hochrein H, Wu L, Shortman K. CD4 and CD8 expression by dendritic cell subtypes in mouse thymus and spleen. *J Immunol* (2000) 164(6):2978–86. doi: 10.4049/jimmunol.164.6.2978
46. Salio M, Cella M, Suter M, Lanzavecchia A. Inhibition of dendritic cell maturation by herpes simplex virus. *Eur J Immunol* (1999) 29(10):3245–53. doi: 10.1002/(SICI)1521-4141(199910)29:10<3245::AID-IMMU3245>3.0.CO;2-X
47. Engelmayer J, Larsson M, Subklewe M, Chahroudi A, Cox WI, Steinman RM, et al. Vaccinia virus inhibits the maturation of human dendritic cells: A novel mechanism of immune evasion. *J Immunol* (1999) 163(12):6762–8. doi: 10.4049/jimmunol.163.12.6762
48. Chang WL, Baumgarth N, Yu D, Barry PA. Human cytomegalovirus-encoded interleukin-10 homolog inhibits maturation of dendritic cells and alters their functionality. *J Virol* (2004) 78(16):8720–31. doi: 10.1128/JVI.78.16.8720-8731.2004
49. Manh TP, Alexandre Y, Baranek T, Crozat K, Dalod M. Plasmacytoid, conventional, and monocyte-derived dendritic cells undergo a profound and convergent genetic reprogramming during their maturation. *Eur J Immunol* (2013) 43(7):1706–15. doi: 10.1002/eji.201243106
50. Renneson J, Dutta B, Goriely S, Danis B, Lecomte S, Laes JF, et al. IL-12 and type I IFN response of neonatal myeloid DC to human CMV infection. *Eur J Immunol* (2009) 39(10):2789–99. doi: 10.1002/eji.200939414

# DuEPublico

Duisburg-Essen Publications online

UNIVERSITÄT  
DUISBURG  
ESSEN

*Offen im Denken*

ub | universitäts  
bibliothek

This text is made available via DuEPublico, the institutional repository of the University of Duisburg-Essen. This version may eventually differ from another version distributed by a commercial publisher.

**DOI:** 10.3389/fimmu.2023.1192057

**URN:** urn:nbn:de:hbz:465-20240614-115809-4



This work may be used under a Creative Commons Attribution 4.0 License (CC BY 4.0).